RESEARCH PAPER

Mechanical Properties of Glass-Ionomer Cement Composed of ZrO_2 and $CaMgSi_2O_6$

Farzaneh Sadat Teimoory[1], Alma Kalali[1], Arvin Attarinavab[2], Mohadeseh Reyhani[1], Hamidreza Rezaie[1,*], Jafar Javadpour[1]

* *hrezaie@iust.ac.ir*

[1] School of Metallurgy and Materials Engineering, Iran University of Science and Technology, Tehran, Iran
[2] Research Department of Nano-Technology and Advanced Materials, Materials and Energy Research Center, Karaj, Iran

Received: April 2025 **Revised: June 2025** **Accepted: July 2025**
DOI: 10.22068/ijmse.3990

Abstract: *Glass ionomer cements (GICs) are widely utilized in clinical restorative dental applications, which suffer from poor mechanical strength. Recent research indicates that GIC achieves optimal performance when modified with a lower percentage of filler materials, particularly when using nanoparticles, due to the resultant increase in surface area and packing density of the cement. Notably, while some fillers enhance the mechanical properties of the cement, others fail to provide improvements. This study addressed a gap in the literature by investigating the impact of acidic/basic additives, such as diopside ($CaMgSi_2O_6$) and zirconia (ZrO_2), on the properties of the cement. The reactivity of zirconia and diopside differs distinctly from traditional calcium-aluminosilicate glass when exposed to acidic conditions in GICs. Also, to clarify the impact of filler's acidity/basicity on filler reactivity during cement setting, the potential for mechanical enhancement by using nano-sized particles is generally limited to the submicron scale. This research incorporated diopside at concentrations of 2, 4, and 6 wt.%, and zirconia at concentrations of 8, 10, and 12 wt.% into a glass powder component. Results demonstrated that adding 8 wt.% zirconia led to a 49% enhancement in compressive strength, also improving microhardness by 16%, attributed to its non-reactive nature, minimal dissolution, and high inherent strength of ZrO_2. In contrast, diopside had a detrimental effect due to its basic nature compared to that of glass powder. The base cement exhibited a setting time of 6.5 min, which slightly increased to 7.4, 7.6, and 7.9 min with the addition of 8, 10, and 12 wt.% zirconia, respectively, while diopside additions at 2, 4, and 6 wt.% resulted in more pronounced increases to 8.3, 8.7, and 9.1 min. Zirconia showed better potential as a reinforcing filler, while diopside, due to its basicity, was less effective in enhancing mechanical performance.*

Keywords: *ZrO_2, Diopside, Glass ionomer cements, Mechanical properties, Dental materials.*

1. INTRODUCTION

Nowadays, various solutions are available for treating and repairing teeth. In the 1900s, Amalgam was the first and strongest dental cavity-filling material, which was composed of Hg, Sn, Ag, and Cu [1-3]. However, two major drawbacks of using amalgam in dental restoration are its improper appearance and weakness in adherence to tooth tissue, as well as corrosion, which rarely causes mercury toxicity [2, 4]. Recently, due to the emphasis on the aesthetic appeal of teeth, patients have begun to prefer materials that are compatible with natural tooth anatomy [5, 6]. Therefore, due to patient demand, scientists consider glass ionomer cement (GIC) and dental composites as more suitable options for both functionality and appearance. Dental cement, after amalgam and composites [7], is the third important category of dental repairing materials [8]. The cements are combinations of powder and liquid that convert to a pasty substance and are used as fillers for cavity and caries repair. The most important dental repairing cements are GICs [9]. The competitive advantages of contemporary GICs compared to other materials include the sustained release of fluoride ions [10], a similarity in thermal expansion coefficient to that of enamel and natural dentin, good chemical and physical adhesion, and biocompatibility [11, 12]. In any case, the primary defect of this restorative dental material is its low mechanical strength compared to the standards of dental materials applications [11].

Traditional GICs are formed through an acid-base reaction between aluminium silicate, alkaline earth-bearing glass powder, and an aqueous solution of polyacrylic acid (PAA) [13]. The formation of a strong three-dimensional (3D) network within the GIC matrix is crucial for achieving high mechanical strength.

Some studies have investigated the effect of reinforcing fillers on GICs to improve their

[DOI: 10.22068/ijmse.3990]

mechanical strength. Different strategies have been suggested, including the use of fibers [11, 14], nanoparticles [15, 16], and even micron-sized additives [17, 18]. Beyond the intrinsic properties of reinforcing particles, their nanoscale dimensions offer advantages such as increased surface area, improved void filling, and enhanced crack resistance [19]. However, the interaction between nanoscale particle size and material properties leads to complex behaviors, making outcomes difficult to predict. Therefore, it is essential to evaluate the overall mechanical performance of GIC composites with micron-sized reinforcing particles. The evidence suggests that incorporating micron-sized ceramic powders can have varying effects on the compressive strength of GICs, with most studies demonstrating enhanced flexural strength [18, 20-22]. Predicting mechanical outcomes remains a significant challenge, as the mechanical outcomes largely depend on the type, size, and concentration of the filler used [11, 22]. These findings emphasize the importance of investigating the intrinsic properties of fillers—particularly their reactivity during the cement setting process. The setting reaction in GICs is governed by an acid–base interaction, in which different materials exhibit varying reactivity rates, affecting the kinetics and final structure of the cement matrix. Incorporating micron-sized ceramic powders with high mechanical strength, such as yttria-stabilized zirconia (YSZ)/ZrO_2, into the glass powder of the cements and other dental materials offers a promising alternative to amalgam due to their superior strength and aesthetic properties [18, 23]. Meanwhile, some studies have shown that GICs reinforced with high hardness and strength micron-sized ceramic powders did not significantly increase the mechanical strength of the GIC composites [18, 22, 24]. The strength of the resulting cement is highly dependent on the acidity/basicity or neutral of the composite materials added compared to the base glass powder. This is because the cement's structure relies on an acid-base reaction, and the nature of the added materials can significantly impact the formation and integrity of the cement network [25]. Zirconia can exhibit acidic, basic or neutral inherent properties depending on the conditions and the other materials it interacts with [26].

Diopside ($CaMgSi_2O_6$) is another moderately strong mineral with good hardness [27]. It is also an important bio-ceramic that contains calcium, magnesium, and silicon with a monoclinic structure [28, 29]. It has been demonstrated to have enhanced bioactivity of the bone cement, with no signs of toxicity [29, 30]. Diopside is generally considered a basic ceramic material because it contains calcium oxide and magnesium oxide in its structure. Due to its biocompatibility and mechanical properties, diopside is used in a wide range of clinical applications including bone [29] and tooth root implants [31], and drug delivery [32].

The size of the reinforcing material is very important. Agglomeration of materials at the nanoscale leads to less precise control over size distribution [33]. Therefore, the addition of zirconia and diopside powders in submicron sizes, close to the nanoscale, was proposed as a reinforcing material for GICs based on their acidic/basic behaviour. Diopside exhibits a slight basic nature due to the presence of alkaline earth metal oxides, while aluminosilicate glass powder and zirconia are amphoteric, capable of reacting with both acids and bases [34-36].

This study investigated the effects of incorporating different percentages of submicron diopside and zirconia particles into GIC. The primary objective was to evaluate the impact of these additives on the mechanical properties of the resulting composite material. For this purpose, a glass ionomer powder based on a SiO_2-Al_2O_3-CaF_2 glass system was synthesized using the melt-quenching method. Diopside powders were synthesized via the sol-gel process. Subsequently, varying amounts of diopside (2, 4, and 6 wt.%) and zirconia (8, 10, and 12 wt.%) were incorporated into the glass powder as reinforcing materials. The mechanical properties of the prepared samples, including compressive strength and microhardness, were evaluated. Additionally, FTIR analysis and pH changes were performed on the resulting cements to facilitate a more thorough investigation and to elucidate the role of reinforcing particles within the cement matrix following the acid-base reaction between the polymer and powders. Furthermore, SEM images examine the morphological features and surface characteristics of the composite cement specimens.

2. EXPERIMENTAL PROCEDURES

2.1. Materials

The raw materials used to synthesize the glass

[DOI: 10.22068/ijmse.3990]

powders were high-grade SiO_2, Al_2O_3, NaF, P_2O_5, CaF_2, and TiO_2, all powders supplied by Merck Co with purities exceeding 99%. The reinforcing powders used in this research were purchased zirconia (ZrO_2, 99.6% Merck, 1314-23-4) and synthesized diopside ($CaMgSi_2O_6$).
Magnesium chloride hexahydrate ($MgCl_2.6H_2O$, 99% Sigma-Aldrich, 7791-18-6) and calcium nitrate tetrahydrate ($Ca(NO_3)_2.4H_2O$ 99% sigma-aldrich, 13477-34-4) were the initial materials for synthesizing diopside by the sol-gel method. Acrylic acid (AA, Merck, 79-10-7), maleic acid (MA, Merck, 110-16-7), potassium persulfate ($K_2S_2O_8$, 99% Merck, 7727-21-1) and ethyl acetate ($CH_3COOC_2H_5$, 99% Merck, 141-78-6) were utilized for synthesizing polymeric acid.

2.2. Synthesis of the Glass Powder

The glass components were weighed meticulously, following the composition derived from the Fuji II commercial powder using XRF analysis, as outlined in Table 1. However, SrF_2 was substituted with CaF2 in the composition of the glass synthesised in this study. Following this, the mixture of oxides and fluorides was heated from room temperature and gradually increased to 1500°C at a heating rate of 7°C/min. The resulted melt was soaked at this elevated temperature for 2h to facilitate homogeneity. Finally, the molten glass was rapidly cooled in distilled water.

2.3. Filler Materials

Zirconia and diopside powders were used as reinforcing fillers in this study. Diopside powder with a submicron particle size was synthesized via the sol-gel method and subsequently processed by planetary milling. The resulting powder exhibited high phase purity, as confirmed by XRD analysis, and displayed a particle size distribution comparable to that of the commercial ZrO_2 filler.

2.4. Co-Polymer Synthesis

The polymer binder was synthesized according to a procedure described in detail by Teimoory Toufal et al [37]. A polymer synthesis experiment began with the preparation of an initiator solution by dissolving $K_2S_2O_8$ in deionized water (DI). The reaction setup involved a three-neck reactor under inert conditions, maintained at 98°C. A solution containing a 8:1 ratio of acrylic acid and maleic acid in DI, along with a $K_2S_2O_8$ solution, was gradually added to the heated initiator solution using a dropping funnel. Following the complete addition, the polymerization reaction continued for 10h. Finally, the polymer product was purified through methanol dissolution followed by precipitation with $CH_3COOC_2H_5$ and freeze drying.

2.5. Cement Sample Preparation of GIC Composites

All GIC composites were prepared manually by mixing the synthesized glass, ZrO_2/diopside powder, and the polymer liquid with a spatula and the resulting paste was set in a mold for 30 min, as described in our previous study [38]. Seven groups of composite cements, each comprising five samples (a total of 35 samples), were created and coded as shown in Table 2. The 0% DIO/ZrO_2 group was considered the control sample (without adding reinforcing powder). The other six groups contain ZrO_2 or diopside particles composited with the glass ionomer powder. Figure 1 presents a schematic illustration of the fabrication process of the glass ionomer cement, including the filler materials, mixing with the polyacrylic acid, and final cement preparation.

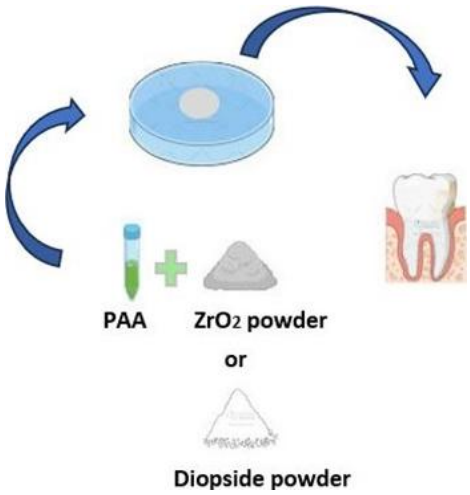

Fig. 1. The schematic illustration of the fabrication method of glass inomer cement

Table 1. The proportions of oxidation and fluoride compounds related to glass composition

Composition	Al_2O_3	SiO_2	NaF	P_2O_5	TiO_2	SrF_2	CaF_2
Fuji II-self cure	25.05	34.4	3.3	4.5	0.23	32.5	-
Glass	25.05	34.4	3.3	4.5	0.23	-	32.59

[DOI: 10.22068/ijmse.3990]

Table 2. Coding are referred to in the context of cement composites and reinforcements containing diopside and ZrO_2

Code Sample	Ca-Cement	2Dio-Ca-Cement	4Dio-Ca-Cement	6Dio-Ca-Cement	8ZrO_2-Ca-Cement	10ZrO_2-Ca-Cemet	12ZrO_2-Ca-Cemet
wt.% of filler	0	2	4	6	8	10	12

2.6. Characterization

The properties of as-quenched glass powders were examined using X-ray diffraction (XRD) and X-ray fluorescence (XRF) analysis to assess compositional changes. The diffraction data were collected using a Cu-Kα radiation diffractometer (D8 Advance, Bruker Kanagawa, Japan) operating at 20 kV and 10 mA. Additionally, scanning electron microscopy (SEM) and simultaneous thermal analysis (STA) were employed for further evaluation. A powder-to-liquid ratio of 1.5 was used to prepare the composite GIC composites. The setting time of the cement formulations was also measured using a Gillmore needle apparatus according to ISO 9917-1:2007 standards. For each composition, three specimens were tested, and the average setting time was reported. Compressive strength was evaluated after 24h of immersion in distilled water. According to ISO 99171:2007 guidelines, specimens prepared for compressive strength testing are 6 mm in height and 4 mm in diameter. Also, the surface morphology of the zirconia-reinforced samples was examined using scanning electron microscopy (SEM). Moreover, samples intended for microhardness testing had dimensions of 6 mm in diameter and 2 mm in height. Vickers hardness measurements were performed using a digital microhardness tester (Matsuzawa, MXT70, Japan) with an applied load of 100 grams for 10 seconds. The hardness value obtained for each sample is an average result of three different points on the surface.

3. RESULTS AND DISCUSSION

3.1. XRD Results

Figure 2 (a) and (b) show the XRD patterns of the purchased zirconia and synthesized diopside powders, respectively.

The prominent peaks observed in this pattern are characteristic of the monoclinic phase of zirconia, which is its most stable polymorph at room temperature. The positions and relative intensities of these peaks are consistent with the JCPDS reference data for monoclinic ZrO_2 in the JCPDS Card (01-078-0091), confirming the phase purity and crystallinity of the as-received zirconia material. The XRD patterns of synthesized DIO exhibit a notable peak at 2θ=30° and another significant peak at approximately 36°, which is consistent with the characteristic peak of DIO reported in the JCPDS reference card (96-101-1048).

3.2. Particle Size and Microstructure of Composite

Particle size plays a crucial role in determining the performance of composite materials, particularly in cement-based systems [39, 40]. The filler particles in most studies are smaller than 100 nm or in the micron range [16].

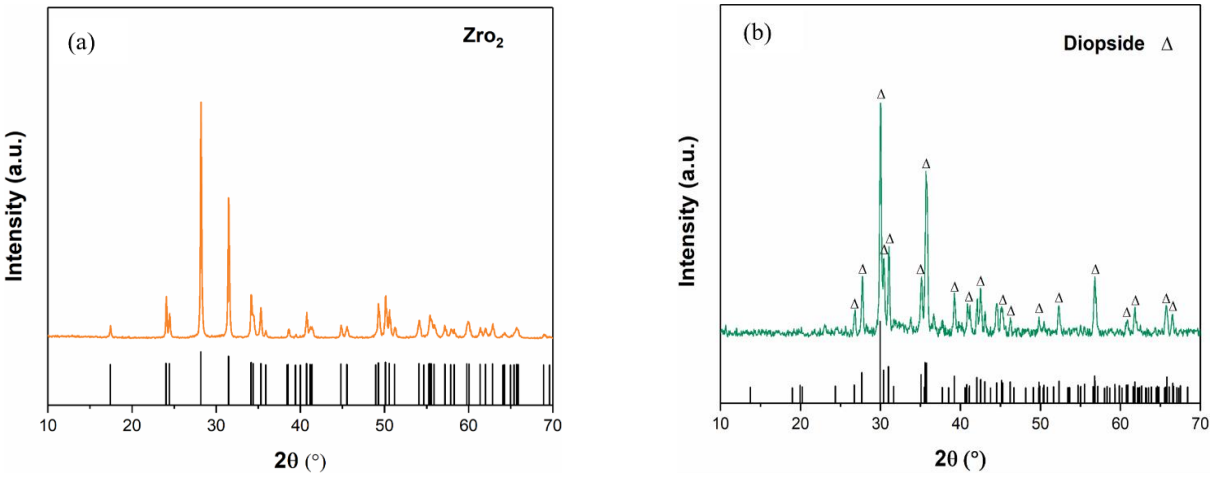

Fig. 2. XRD patterns of a) purchased zirconia (ZrO_2) and b) synthesized diopside ($CaMgSi_2O_6$)

[DOI: 10.22068/ijmse.3990]

The frits and diopside were grinded for 3h in the zirconia cup at 300 rpm in a planetary mill (pm 400, Retch, Germany) the resulted powders were examined using the particle size analyzer (PSA). Figure 3-a shows the SEM image of as-milled glass powders. PSA result is depicted in Figure 3-b. The results revealed that the glass particles range within the 1-10 µm.

The dynamic light scattering (DLS) method was employed to determine the median size of the synthesized diopside post-milling and sieving and the as-milled zirconia particles which was in the range of approximately 220 and 200 nm, respectively (Figure 3-c and d).

Beyond particle size, understanding the internal structure and chemical environment of the glass is critical for predicting its reactivity and performance in GICs. Calcium aluminosilicate (CAS) glasses contain both bridging oxygen (BO) and non-bridging oxygen (NBO) ions that define their structure [41, 42]. Studies indicate that fluoride-substituted oxygen tends to bond with modifiers in high-fluoride glasses [43]. Conversely, 19F and 29Si NMR analysis revealed poor bonding between fluorine and silicon, thereby increasing the likelihood of F-bonding with calcium and aluminium compared to Si-F bonding [44]. Additionally, the glass in this study exhibited an amorphous-amorphous/crystalline phase separation, which may result in nanoscale heterogeneities or localised crystalline regions within the amorphous matrix [37].

Figure 4 illustrates the SEM images and EDS analysis of the etched first glass surfaces, which reveal the limited formation of fluorine-rich crystalline zones on the glass particle surfaces. Although the percentage of separated phases was not as high as indicated in the XRD analysis, the presence of these phases in the synthesized glass can positively affect the cement by reducing its setting time. In this way, it improves acid hydrolysis, leading to increased reactivity of the glass powder with acid. This separation facilitates the availability of participating elements to cross-link with the polymeric matrix during the setting stage of cement.

3.3. Thermal Behavior of the Glass

Figure 5 illustrates the thermal behavior of the glass powder.

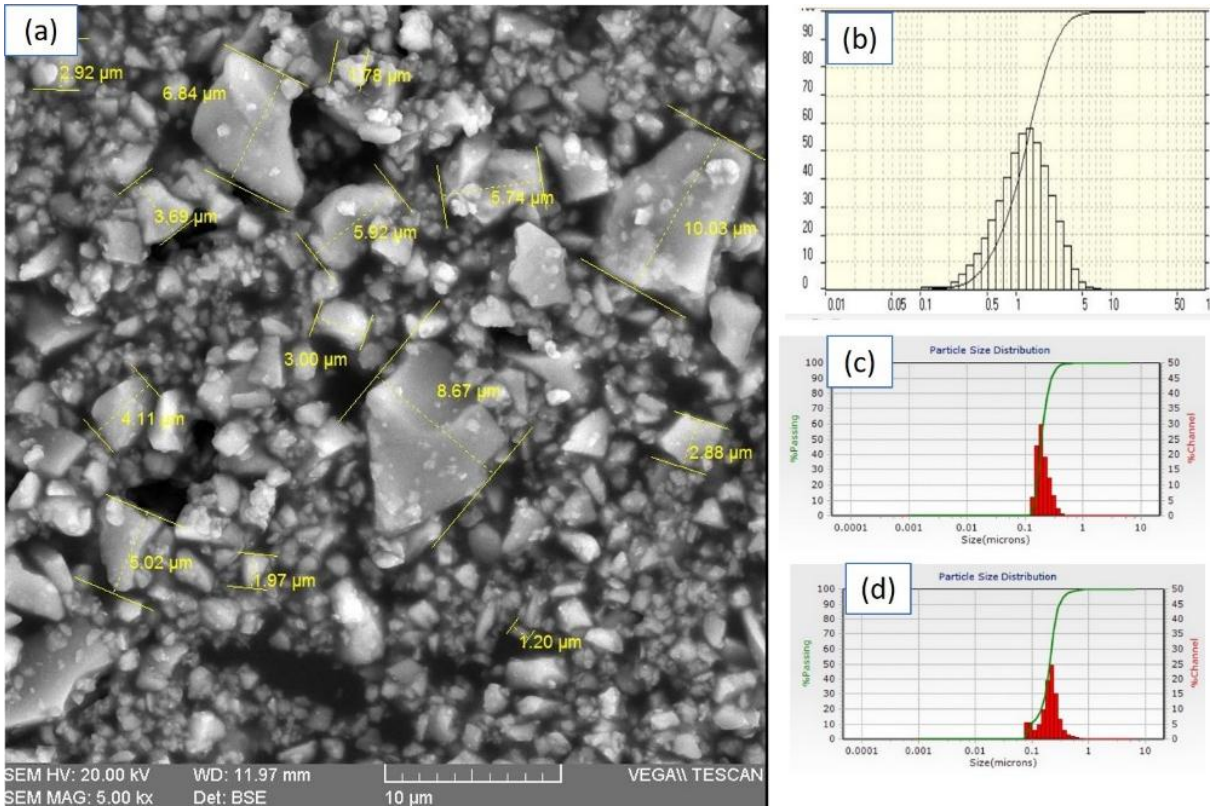

Fig. 3. a) SEM image of melted and milled glass particles b) PSA analysis of synthesized glass particles c) DLS analysis of synthesized diopside particles d) DLS analysis of purchased zirconia powders

[DOI: 10.22068/ijmse.3990]

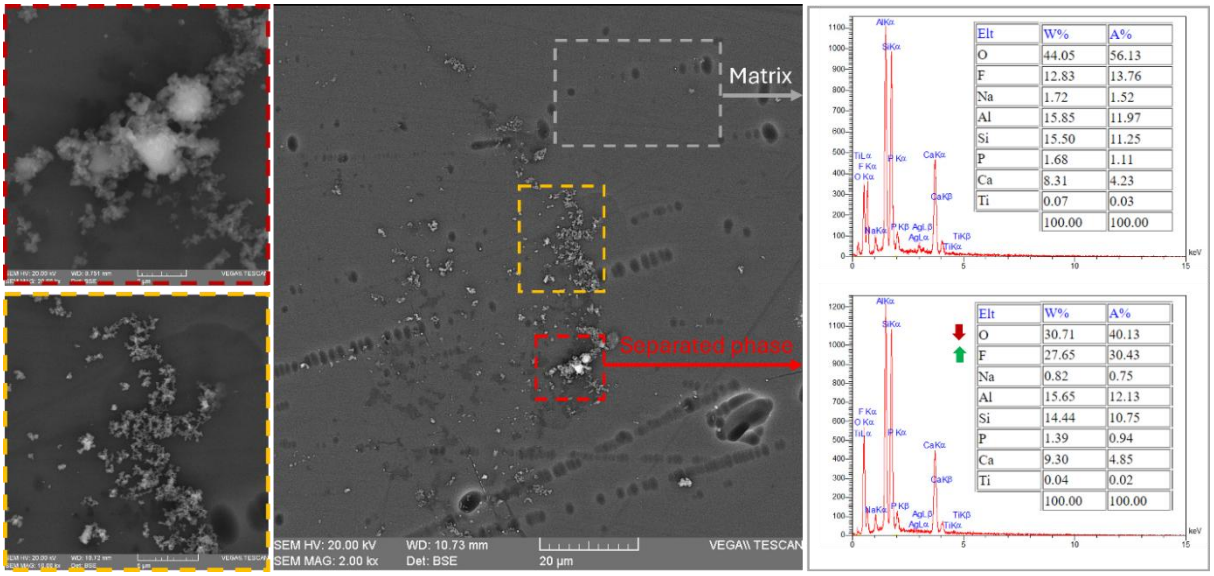

Fig. 4. Examination of etched glass surfaces and observation of fluorine-rich isolated phases by SEM and EDX analysis

The glass transition temperature (T_g) is observed at 510°C, followed by a broad exothermic peak around 850°C. Heating the glass to 850°C for 15 min resulted in the formation of calcium anorthite crystalline phases, as confirmed by XRD analysis (Figure 5-b) [42]. It is important to distinguish between glasses with a stoichiometric anorthite composition (amorphous) and crystalline anorthite ($CaAl_2Si_2O_8$), as their reactivity, particularly with organic acids in glass ionomer cements, differs significantly. However, it is pertinent to note that the overall chemical composition of our glass, when plotted on the relevant CaO-Al_2O_3-SiO_2 phase diagram, falls within the primary crystallization field of anorthite, which explains its formation upon thermal treatment. While literature suggests that glasses with a bulk anorthite composition may exhibit longer setting times in glass ionomer cements compared to gehlenite glass compositions, the specific impact of the observed anorthite crystallization on the reactivity of this particular glass requires further investigation [45].

3.4. The Setting Time of GICs

The setting time of glass ionomer cements (GICs) is a crucial clinical property that influences workability. In this study, the base cement (control) exhibited a setting time of 6.5 min. Interestingly, the addition of both zirconia and diopside fillers led to an increase in setting time, albeit to varying degrees. For zirconia-modified cements, the setting time slightly increased to 7.4, 7.6, and 7.9 min with the addition of 8, 10, and 12 wt.% zirconia, respectively. This observed increase is primarily attributed to the barrier effect of the zirconia particles.

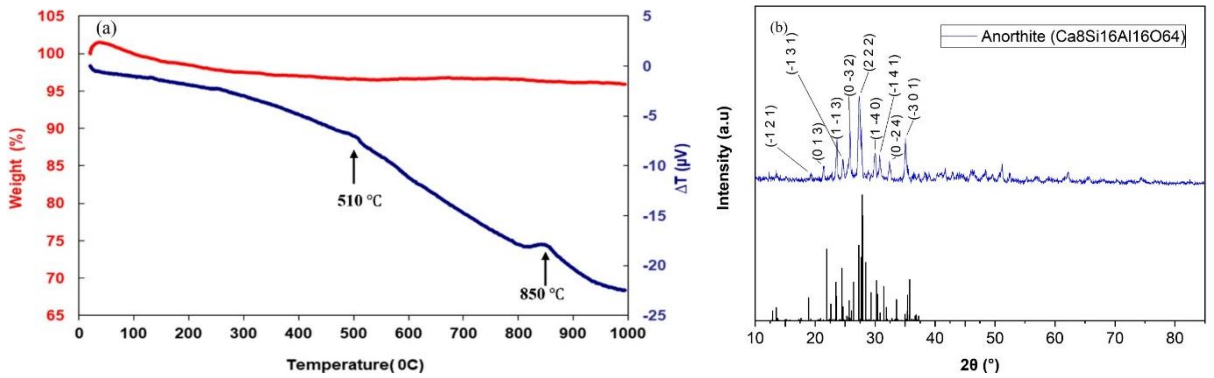

Fig. 5. a) Differential thermal and thermogravimetric analysis curves of Ca-Glass, b) X-ray diffraction pattern of heat-treated glass at 850°C for 15 minutes

[DOI: 10.22068/ijmse.3990]

Zirconia, being chemically stable and relatively inert in the acidic GIC environment, physically obstructs the direct contact between the active glass particles and the polyacrylic acid solution. This impedes the initial acid-base reaction, which is fundamental for ion release and the subsequent cross-linking process, thereby prolonging the overall setting time.

In contrast, diopside additions resulted in more pronounced increases in setting time, reaching 8.3, 8.7, and 9.1 minutes for 2, 4, and 6 wt.% additions, respectively. Similar to zirconia, diopside particles can also exert a physical barrier effect, hindering the direct interaction between the glass and polyacid. However, diopside's impact on setting time is further exacerbated by its basic nature. Beyond the physical impedance, the basicity of diopside leads to a partial neutralization of the polyacrylic acid, which is essential for dissolving the glass and initiating ion release. This premature neutralization directly interferes with the acid-base reaction kinetics, limiting the optimal release of cross-linking ions (like Al^{3+} and Ca^{2+}) from the main glass powder. Consequently, the formation of the robust 3D polyacrylate network is delayed, resulting in a more significant increase in the setting time compared to zirconia.

The distinct influences of zirconia and diopside on setting time highlight the complex interplay between filler particle properties (inertness vs. reactivity, physical vs. chemical effects) and the intricate acid-base setting mechanism of GICs.

3.5. The Mechanical Properties of GIC

According to ISO 9917-1:2007, the compressive strength (CS) and microhardness (HV) tests are recognized as suitable criteria for evaluating the strength of GICs. Compressive strength is defined as the maximum stress a material can withstand without failing. This measure is widely utilized as a method for assessing the strength of dental cement materials, including GICs. In this study, the mechanical properties of composite cement according to Table 2 with the addition of 2, 4 and 6 wt.% diopside powder, as well as composite cement with 8, 10, and 12 wt.% zirconia powder, were examined. Compressive strength and hardness were measured from the optimal percentages of composites with zirconia and diopside.

The average compressive strength results of various cement groups are presented in Figure 6, measured after 24h of setting. The control sample demonstrated a baseline strength of 44.08 MPa. Among the zirconia-based composites, the $8ZrO_2$-Ca-Cement formulation achieved the highest compressive strength of 65.9 MPa, representing a 49% improvement over the control sample. Notably, all zirconia-containing glass ionomer cements GICs exhibited superior strength compared to the control group. In contrast, the diopside composites showed varying strengths ranging from 14.5 to 44.02 MPa across different concentrations (2, 4, and 6 wt.%). Within this group, the 2DIO-Ca-Cement formulation achieved the highest compressive strength. However, unlike zirconia, the addition of diopside did not demonstrate a positive effect on composite strength.

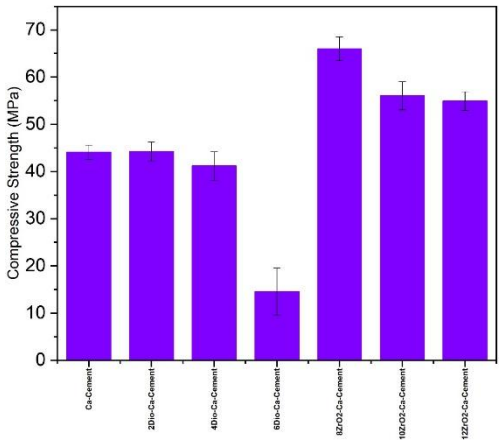

Fig. 6. The compressive strength of cement samples containing diopside and zirconia measured after immersing in distilled water for 1 day

While the absolute compressive strengths obtained are lower than typical commercial GICs (e.g., Fuji II, which can exceed 168 MPa at 24h), this is primarily attributed to the properties of our synthesized polyacrylic acid (PAA) polymer. An experiment combining commercial Fuji II glass powder with our PAA yielded approximately 75 MPa at 24h, suggesting that the lower molecular weight of our PAA, compared to proprietary commercial polymers, significantly impacts the overall cement strength. Despite this, the observed trends and relative improvements with zirconia and diopside additions remain valid within our experimental system, guiding future optimization towards higher molecular weight polymer synthesis.

Previous research has demonstrated that incorporating zirconia nanoparticles, particularly those less than 100 nm, improves the mechanical

[DOI: 10.22068/ijmse.3990]

properties of GICs [46, 47]. Studies have conclusively established that most ceramic nanoparticles contribute to enhanced strength characteristics primarily by reducing the porosity and inducing crack deflection mechanisms [48, 49]. Conversely, certain investigations have revealed limitations associated with the aggregation of nanometer-scale materials, resulting in diminished control over particle size distribution and consequently resulting the detrimental effect of zirconia-based composites [47, 48]. Furthermore, there is a lack of experimental data examining the compressive strength attributes of submicron GICs incorporating zirconia powder. Some Studies has indicated that zirconia within the submicron (spanning 1 µm to 10 µm) can enhance the mechanical properties [47, 48]. However, other findings suggested that increasing the percentages of nano-micron zirconia may less positively affect the improvement of compressive strength characteristics [47]. This phenomenon can be attributed to various factors. Generally, higher percentages of the second phase tend to increase accumulation and clustering, often leading to increased porosity in the composite structure. Such porosity can serve as a nucleation site for crack formation under applied forces [48]. Furthermore, elevating the volume fraction of zirconia may extend the duration of the cement setting and facilitate the formation of insufficient cross-link bonds within its polymer chains. Diopside contains high levels of magnesium and calcium cations that can contribute to cement reactions and exhibits a more basic nature compared to both calcium-aluminosilicate glass powder and zirconia [26].

3.6. Scanning Electron Microscopy (SEM)

Scanning electron microscopy (SEM) analysis of the composite materials reveals distinct variations in zirconia particle distribution. The $8ZrO_2$-Ca-Cement formulation demonstrates optimal zirconia particle dispersion across the surface. However, SEM examination of specimens containing 10 and 12 weight percent zirconia reveals evidence of particle agglomeration on the surface (Figures 7c and 7d).

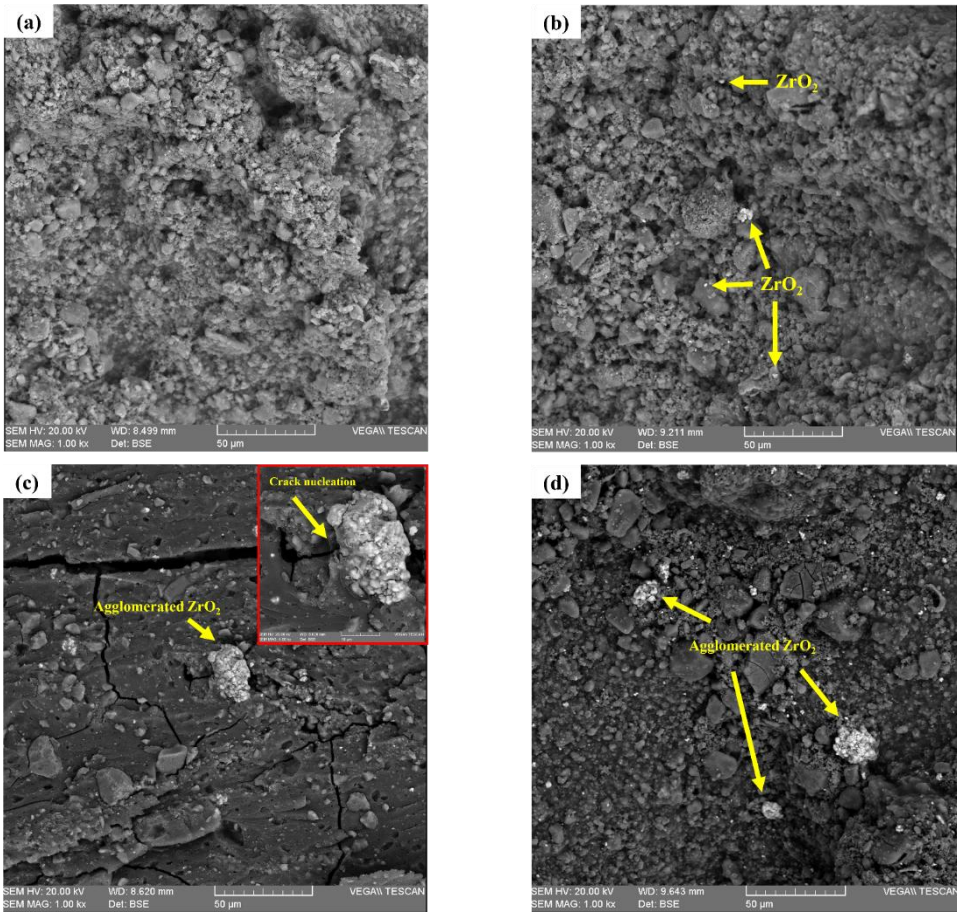

Fig. 7. SEM image of composites: a) Ca-Cement, b) $8ZrO_2$-Ca-Cement, c) $10ZrO_2$-Ca-Cement, d) $12ZrO_2$-Ca-Cement

[DOI: 10.22068/ijmse.3990]

As illustrated in Figure 7c, the formation of larger zirconia agglomerates creates potential crack initiation sites under compressive loading. Furthermore, as the zirconia content increases in the composite formulation, particle distribution becomes progressively compromised, leading to increased accumulation of zirconia particles.

3.7. FTIR Results

The correlation between the intensity of symmetrical and asymmetrical cross-links formed and cement strength was studied via FTIR spectroscopy. The spectra of samples, specifically within the 1300-1800 cm^{-1} range, are presented in Figure 8. The symmetrical and asymmetrical cross-links formed arise from the interaction between aluminum and calcium ions with COO^- functional group during the setting reaction. Absorbtion bands of 1469 and 1619 cm^{-1} are associated with symmetric and asymmetric aluminum carboxylate compounds, respectively [25, 50]. In 4Dio-Ca-Cement (red), the reduced intensity of these aluminum carboxylate bands, compared to Ca-Cement (green) and $10ZrO_2$-Ca-Cement (black), indicates a diminished formation of aluminum carboxylate cross-links. Moreover, calcium carboxylate absorption symmetric and asymmetric bands are 1415 and 1574 cm^{-1} [25]. Furthermore, the lower intensity of symmetric and asymmetric Ca- COO^- bonds in 4Dio-Ca-Cement, compared to Ca-Cement, indicates a lower degree of cross-linking within the cement matrix [38, 50, 51].

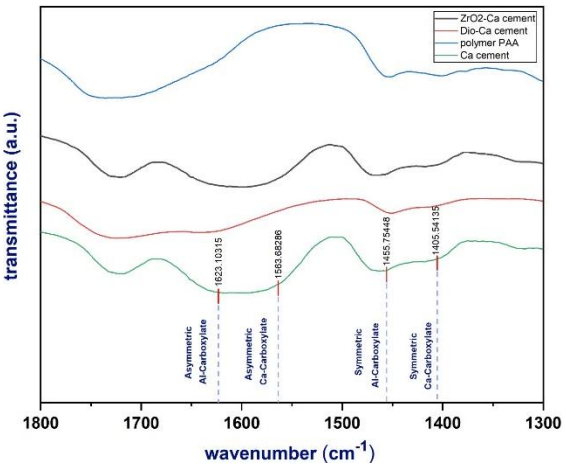

Fig. 8. FTIR spectra of GICs containing: PAA polymer (blue), Ca-Cement (green), 4Dio-Ca-Cement (red), and $10ZrO_2$-Ca-Cement (black)

The overall diminished salt-carboxylate network (COO^- Ca^{2+} and COO^- Al^{3+}) in diopside-modified cement is a direct consequence of diopside's basicity. This basic nature interferes with the setting reaction by partially neutralizing the polyacid and thus limiting the critical ion release from the glass powder, hindering the complete formation of the robust 3D polymer-salt network. In contrast, zirconia's neutral nature allows for proper network development. Diopside's rapid ion release also disrupts the glass-acid reaction, delaying setting and weakening initial cement strength [52].

3.8. The Microhardness of the Cement

The wear resistance of dental restorative materials in the actual oral environment can be assessed using the microhardness test as a criterion. The microhardness data of GIC samples are illustrated in Figure 9 which were measured according to the ISO 9917-1:2007 standard. In ZrO_2-Ca-cements, a significant increase in hardness can be seen compared to Ca-cements. This is likely due to the inherently harder nature of zirconia particles than glass particles, suggesting that a higher concentration of zirconia results in a harder material.

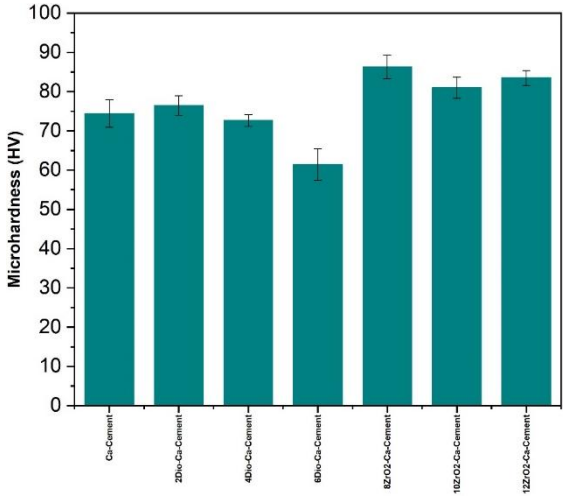

Fig. 9. Microhardness measurements of GIC reinforced with varying concentrations of zirconia and diopside nanoparticles

Also, adding 2% diopside to the glass ionomer resulted in a slight increase in hardness than Ca-cement. However, a decrease in hardness was observed upon further increasing the amount of Diopside and zirconia in the composite composition of the glass ionomer. On the other hand, it is believed that the reduction in micro-hardness due to an excess of diopside particles suggests insufficient bond between the PAA

[DOI: 10.22068/ijmse.3990]

polymer and glass particles. This phenomenon can be attributed to the number of carboxylic acid groups available for bonding with glass particles. As the percentage of diopside particles increases, cracks around these nanoparticles become more prevalent. Consequently, the number of cracks in the interface also increases, resulting in a significant drop in microhardness.

4. CONCLUSIONS

This study aimed to develop GICs with enhanced mechanical properties for restorative dental applications. To achieve this, the effects of incorporating different percentages of zirconia and diopside nanoparticles (refer to Table 2) into the cement matrix were investigated. The results demonstrated that zirconia significantly improved the compressive strength of the GIC and 8 wt.% zirconia yielded a 46% increase in strength. This enhancement can be attributed to the more acidic nature of zirconia compare to glass powder, which facilitated stronger interfacial bonding within the cement matrix. In contrast, diopside, with its more basic nature, did not significantly improve the mechanical properties. Also, less bonds between the PAA and the Dio-Ca glass than ZrO_2-Ca glass because of their basic nature, resulted in weaker microhardness. Regarding setting time, both zirconia and diopside additions resulted in a longer setting time for the GICs. Zirconia primarily acted as a physical barrier, slightly impeding the acid-base reaction. Diopside, however, caused a more pronounced increase in setting time due to its basicity, which interfered with the acid-base reaction kinetics by neutralizing the acid and limiting ion release, thereby hindering optimal network formation.

These findings highlight the crucial role of the acid-base properties of additives in determining the overall mechanical performance of GICs. Further research is needed to optimize the selection and incorporation of reinforcing agents for improving clinical outcomes.

REFERENCES

[1] R. Bharti, K.K. Wadhwani, A.P. Tikku, A. Chandra, Dental amalgam: An update, Journal of Conservative Dentistry 13(4) (2010) 204-208.

[2] M. Hanson, J. Pleva, The dental amalgam issue. A review, Experientia 47 (1991) 9-22.

[3] N. Bahremandi Tolou, M. H. Fathi, A. Monshi, F.S. V. S. Mortazavi, M. Mohammadi, "The Effect of Adding TiO_2 Nanoparticles on Dental Amalgam Properties", Iranian Journal of Materials Science and Engineering 10(2) (2013) 46-56.

[4] L. Mackenzie, Dental amalgam: a practical guide, Dental Update 48(8) (2021) 607-618.

[5] M. Blatz, G. Chiche, O. Bahat, R. Roblee, C. Coachman, H. Heymann, Evolution of aesthetic dentistry, Journal of dental research 98(12) (2019) 1294-1304.

[6] H.F. Albers, Tooth-colored restoratives: principles and techniques, PMPH-USA2002.

[7] F. Foroutan, J. Javadpou, A. khavandi, M. Atai, H. R. Rezaie, "Mechanical Properties of Dental Composite Materials Reinforced with Micro and Nano-Size Al_2O_3 Filler Particles", Iranian Journal of Materials Science and Engineering 8(2) (2011) 25-33.

[8] R. Hickel, K. Brüshaver, N. Ilie, Repair of restorations–criteria for decision making and clinical recommendations, Dental Materials 29(1) (2013) 28-50.

[9] D.J. Wood, Fundamental studies on ionomer glasses, University of Greenwich, 1993.

[10] J.W. Nicholson, S.K. Sidhu, B. Czarnecka, Fluoride exchange by glass-ionomer dental cements and its clinical effects: a review, Biomaterial Investigations in Dentistry 10(1) (2023) 2244982.

[11] J.W. Nicholson, S.K. Sidhu, B. Czarnecka, Enhancing the mechanical properties of glass-ionomer dental cements: a review, Materials 13(11) (2020) 2510.

[12] G. Pinto-Sinai, J. Brewster, H. Roberts, Linear coefficient of thermal expansion evaluation of glass ionomer and resin-modified glass ionomer restorative materials, Operative Dentistry 43(5) (2018) E266-E272.

[13] U.S.N.G. Saridena, G.S.S.J. Sanka, R.K. Alla, R. AV, S.S. Mc, S.R. Mantena, An overview of advances in glass ionomer cements, International Journal of Dental Materials 4(4) (2022) 89-94.

[14] R.M. Silva, F.V. Pereira, F.A. Mota, E. Watanabe, S.M. Soares, M.H. Santos, Dental glass ionomer cement reinforced by cellulose microfibers and cellulose nanocrystals, Materials Science and Engineering: C 58 (2016) 389-395.

[DOI: 10.22068/ijmse.3990]

[15] S.E. Elsaka, I.M. Hamouda, M.V. Swain, Titanium dioxide nanoparticles addition to a conventional glass-ionomer restorative: influence on physical and antibacterial properties, Journal of dentistry 39(9) (2011) 589-598.
[16] I.A. Moheet, N. Luddin, I.A. Rahman, T.P. Kannan, N.R. Nik Abd Ghani, S.M. Masudi, Modifications of Glass Ionomer Cement Powder by Addition of Recently Fabricated Nano-Fillers and Their Effect on the Properties: A Review, Eur J Dent 13(3) (2019) 470-477.
[17] A. Yap, Y. Pek, R. Kumar, P. Cheang, K. Khor, Experimental studies on a new bioactive material: HAIonomer cements, Biomaterials 23(3) (2002) 955-962.
[18] R. Albeshti, S. Shahid, Evaluation of microleakage in zirconomer®: A zirconia reinforced glass ionomer cement, Acta Stomatologica Croatica 52(2) (2018) 97.
[19] E. Gjorgievska, J.W. Nicholson, D. Gabrić, Z.A. Guclu, I. Miletić, N.J. Coleman, Assessment of the Impact of the Addition of Nanoparticles on the Properties of Glass–Ionomer Cements, Materials 13(2) (2020) 276.
[20] R.M. Silva, F.V. Pereira, F.A. Mota, E. Watanabe, S.M. Soares, M.H. Santos, Dental glass ionomer cement reinforced by cellulose microfibers and cellulose nanocrystals, Mater Sci Eng C Mater Biol Appl 58 (2016) 389-95.
[21] A. Bhattacharya, S. Vaidya, A.K. Tomer, A. Raina, GIC at its best–A review on ceramic reinforced GIC, International Journal of Applied Dental Sciences 3(4) (2017) 405-408.
[22] J.W. Nicholson, S.K. Sidhu, B. Czarnecka, Enhancing the Mechanical Properties of Glass-Ionomer Dental Cements: A Review, Materials (Basel) 13(11) (2020).
[23] Y. Gu, A. Yap, P. Cheang, K. Khor, Zirconia–glass ionomer cement—a potential substitute for Miracle Mix, Scripta materialia 52(2) (2005) 113-116.
[24] S. Chen, Y. Cai, H. Engqvist, W. Xia, Enhanced bioactivity of glass ionomer cement by incorporating calcium silicates, Biomatter 6(1) (2016) e1123842.
[25] J.W. Nicholson, Chemistry of glass-ionomer cements: a review, Biomaterials 19(6) (1998) 485-94.
[26] H. Nakabayashi, Properties of Acid and Base Sites on Zirconium Oxides Having Monoclinic and Tetragonal Structures Formed by Calcination at Low Temperature, Nippon Kagaku Kaishi 2000 (2000) 841-849.
[27] M. Smedskjaer, M. Jensen, Y. Yue, Theoretical Calculation and Measurement of the Hardness of Diopside, Journal of the American Ceramic Society 91 (2008) 514-518.
[28] S.N. Salama, H. Darwish, H.A. Abo-Mosallam, HA forming ability of some glass-ceramics of the $CaMgSi_2O_6$–$Ca_5(PO_4)_3F$–$CaAl_2SiO_6$ system, Ceramics International 32(4) (2006) 357-364.
[29] Y.-M. Chang, Y.-S. Tseng, C.-L. Chen, D.A.H. Hanaor, T.-W. Lin, T.-s. Chang, W.-F. Chen, Synthesis and properties of $CaMgSi_2O_6$-SrO bioceramics for enhanced hydroxyapatite formation and cell viability in bone regeneration, Ceramics International 50(24, Part B) (2024) 54320-54334.
[30] A. Kalali, H. Rezaie, S. Hesaraki, M. Khodaei, F. Teimoory, A. Saboori, 3D printing of composite scaffolds based on polycaprolactone matrix reinforced with monticellite and akermanite for bone repair; mechanical and biological properties, Materialia 34 (2024).
[31] M. Razavi, M. Fathi, O. Savabi, S. Razavi, F. Heidari, M. Manshaei, D. Vashaee, L. Tayebi, In vivo study of nanostructured diopside ($CaMgSi_2O_6$) coating on magnesium alloy as biodegradable orthopedic implants, Applied Surface Science 313 (2014).
[32] S. Chidambaram, S. Swamiappan, Bioactive Diopside ($CaMgSi_2O_6$) as a Drug Delivery Carrier–A Review, Current drug delivery 9 (2012).
[33] S. Kumari, S. Raturi, S. Kulshrestha, K. Chauhan, S. Dhingra, K. András, K. Thu, R. Khargotra, T. Singh, A comprehensive review on various techniques used for synthesizing nanoparticles, Journal of Materials Research and Technology 27 (2023) 1739-1763.
[34] V.I. Vereshchagin, V.K. Men'shikova, A.E. Buruchenko, N.V. Mogilevskaya, Ceramic materials based on diopside, Glass and Ceramics 67 (2011) 343-346.

[DOI: 10.22068/ijmse.3990]

[35] M. Grün, A.A. Kurganov, S. Schacht, F. Schüth, K.K. Unger, Comparison of an ordered mesoporous aluminosilicate, silica, alumina, titania and zirconia in normal-phase high-performance liquid chromatography, Journal of Chromatography A 740(1) (1996) 1-9.

[36] M. Alireza, R. Nima, W.L.C. Winston, R.S. Scott, A review of powder modifications in conventional glass-ionomer dental cements, J. Mater. Chem. 21(5) (2011) 1319-1328.

[37] F.S. Teimoory, H.R. Rezaie, B.E. Yekta, J.W. Nicholson, J. Javadpour, Enhancing mechanical strength of Sr-based oxyfluoride glasses in glass ionomer cement through phase separation, Ceramics International 50(14) (2024) 24970-24978.

[38] F.S. Teimoory, H.R. Rezaie, B.E. Yekta, J.W. Nicholson, J. Javadpour, The Role of AlO_x Species in Sr-Aluminosilicate Glasses on the Mechanical Properties of Dental Glass Ionomer Cement Due to Zinc Cation Substitution, Ceramics International (2024).

[39] D. Bentz, E.J. Garboczi, C. Haecker, O. Jensen, Effects of Cement Particle Size Distribution on Performance Properties of Portland Cement-Based Materials, Cement and Concrete Research 29 (1999) 1663-1671.

[40] L.H. Prentice, M.J. Tyas, M.F. Burrow, The effect of particle size distribution on an experimental glass-ionomer cement, Dental Materials 21(6) (2005) 505-510.

[41] M. Turchi, S. Perera, S. Ramsheh, A.J. Popel, D.V. Okhrimenko, S.L.S. Stipp, M. Solvang, M.P. Andersson, T.R. Walsh, Predicted structures of calcium aluminosilicate glass as a model for stone wool fiber: effects of composition and interatomic potential, Journal of Non-Crystalline Solids 567 (2021) 120924.

[42] L. Cormier, Glasses: Aluminosilicates Verres: aluminosilicates, Encyclopedia of Materials: Technical Ceramics and Glasses, Elsevier2021, pp. 496-518.

[43] J. Zhao, X. Xu, X. Qiao, J. Du, Fluoride and Oxyfluoride Glasses, 2022, pp. 439-463.

[44] Tomoaki, Maeda, S. Matsuya, M. Ohta, Effects of CaF_2 Addition on the Structure of CaO-Al_2O_3-SiO_2 Glasses, 2008.

[45] A.D. Wilson, S. Crisp, H.J. Prosser, B.G. Lewis, S.A. Merson, Aluminosilicate Glasses for Polyelectrolyte Cements, Industrial & Engineering Chemistry Product Research and Development 19(2) (1980) 263-270.

[46] K. Jain, J. Paulraj, S. Maiti, R. Shanmugam, Green Synthesis and Investigation of Antimicrobial Activity and Compressive Resilience of Glass Ionomer Cement Modified With Zirconia Nanoparticles: An In Vitro Study, Cureus 16(6) (2024) e62837.

[47] Y. Gu, A. Yap, P. Cheang, Y. Koh, K. Khor, Development of zirconia-glass ionomer cement composites, Journal of Non-crystalline Solids-J Non-Cryst Solids 351 (2005) 508-514.

[48] M. Ghaffari, P. Alizadeh, M.R. Rahimipour, Sintering behavior and mechanical properties of mica-diopside glass–ceramic composites reinforced by nano and micro-sized zirconia particles, Journal of Non-Crystalline Solids 358(23) (2012) 3304-3311.

[49] N. Fazelian, S. Pourarz, K. Yaghmoori, B. Naziri, Effects of incorporation of various amounts of zirconium oxide particles on microstructure and mechanical strength of conventional and light-cure glass ionomer cements, Annals of Medical and Health Sciences Research| Volume 8(6) (2018).

[50] A. Zandi Karimi, Development of glass ionomer cements with improved mechanical and remineralizing properties by incorporation of 45S5 Bioglass®-ceramic, Concordia University, 2019.

[51] A. Karimi, E. Rezabeigi, R. Drew, Aluminum-free glass ionomer cements containing 45S5 Bioglass and its bioglass-ceramic, Journal of Materials Science: Materials in Medicine 32 (2021).

[52] X. Chen, D. Brauer, N. Karpukhina, R. Waite, M. Barry, I. McKay, R. Hill, 'Smart' acid-degradable zinc-releasing silicate glasses, Materials letters 126 (2014) 278-280.

[DOI: 10.22068/ijmse.3990]